

**CONSTRUCTION AND INITIAL OPERATION OF A PROPORTIONAL WIRE DETECTOR
FOR USE IN A CERENKOV RING IMAGING SYSTEM***

J. VA'VRA, T. BIENZ, F. BIRD, M. GAILLARD,[†] G. HALLEWELL, Y. J. KWON
D. LEITH, B. RATCLIFF, P. RENSING, D. SCHULTZ, S. SHAPIRO, N. TOGE

Stanford Linear Accelerator Center, P. O. Box 4349, Stanford, CA 94305

M. CAVALLI-SFORZA, P. COYLE, D. COYNE, D. WILLIAMS

University of California, Santa Cruz, CA 95064

D. CALDWELL, A. LU, S. YELLIN

University of California, Santa Barbara, CA 93106

R. JOHNSON, B. MEADOWS, M. NUSSBAUM

University of Cincinnati, Cincinnati, OH 45221

R. PLANO

Rutgers University, New Brunswick, NJ 08903

Abstract

We report on the final version of the multiwire single electron detector for the Cerenkov ring imaging device at SLD. We describe recent R&D effort to define the design parameters; we describe the details of the geometry of the detector, and experimental tests with the detector itself.

1. Introduction

The detector must have a high efficiency for detecting single photoelectrons produced by Cerenkov photons. The principle of this detector is based on earlier published work.¹ The detector measures the z-coordinate (along the drift box axis) of the photoelectron by measuring the drift time, the radial coordinate (along the drift box height) by measuring the charge division on each anode wire, and the azimuthal coordinate by the wire address. The radial coordinate is essential for reduction of parallax broadening on the Cerenkov ring images. The use of TMAE (tetrakis dimethylamino ethylene), which serves as a photocathode, strongly influences the design parameters of the detector. Although there are many similarities between the SLD CRID and DELPHI RICH devices,² it is the electron detector where the two devices differ rather substantially (in the RICH detectors the radial coordinate is derived from the cathode strip readout). For an up to date review of the overall CRID system, see a paper given at this symposium.³

2. Detector Description

Each CRID electron detector will be instrumented with 93 anode wires on a 3.175 mm pitch. At our operating temperature of $\sim 28^\circ \text{C}$ the photo-ionizing TMAE vapor has an absorption length of about 16 mm, thus the UV photons produced in the avalanche at the proportional chamber wire can travel back into the gas volume and be converted several centimeters away, resulting in a feedback mechanism. The suppression of the photon feedback is realized by the geometry shown in Fig. 1. The walls of the "U" shaped cathode (a nickel plated aluminum block) eliminate the "direct communication"

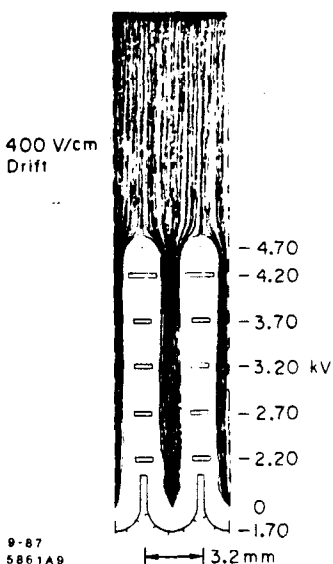


Fig. 1. Electrostatic design of the CRID electron detection ($E_{\text{drift}} = 400 \text{ V/cm}$, $B_z = 6$, $B_r = 0.3 \text{ kg}$, C_2H_6 gas parameters). A number of electron drift trajectories are shown.

between neighboring wires. Five layers of etched copper beryllium sheets (blinds),⁴ each $254 \mu\text{m}$ thick, are stacked above the cathode and limit the angle ($\sim 6.6^\circ$) over which photons from the avalanche can reach the detector volume. Each blind has 93 openings (2 mm wide), each centered above an anode wire. All five blinds are stacked on G-10 spacers and glued together to form an easily removable 15 mm thick package. Before the first blind, there is a wire plane (100 μm Cu-Be wires) which guides the drifting electrons into the openings in the etched sheets. In addition, this wire plane can also serve as a gate to prevent positive ions from reaching the drift volume and photoelectrons from reaching the anode. This is accomplished by pulsed biasing of the odd and even gate wires by $\pm 150 \text{ V}$.⁵ Figure 2 shows a picture of the finished single electron detector for the CRID system.

To achieve the desired 1% position resolution using the charge division technique on single electron signals, it is necessary to reduce the Johnson noise originating in the anode wire. We therefore utilize high resistance carbon fibers of $7 \mu\text{m}$

*Work supported by Department of Energy contracts DE-AC03-76SF00515 and DE-AT03-79ER70023, and by National Science Foundation Grants PHY85-12145 and PHY85-13808.

[†]Present Address: Lab. de L'Accelerateur Linéaire, Batiment 200, F91405 Orsay, Cedex, France

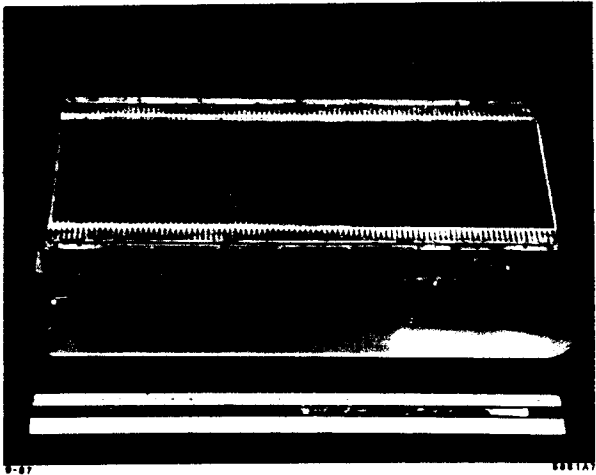


Fig. 2. Completed CRID single electron detector.

diameter. Our amplifier⁶ connected to such a wire has an input noise of about 1100 electrons (rms). Based on results from our physics prototype,⁷ one expects the third coordinate to be measured to 1-2 mm if one operates the wire gain in a region of 2×10^5 total gain.

The detector is optimized for single electron detection. However, it will also detect the large dE/dx ionization loss from charged particles, thus, very large signals, equivalent to up to 1000 primary electrons, will be observed. To minimize the resulting crosstalk we have incorporated shielded signal traces between the wire and the amplifier input, and have tried to keep the signal to ground capacitance as low as possible to minimize the amplifier noise. The measured value of this capacitance for the final detector (including the anode wire) is about 6 pF/channel. The magnitude of the crosstalk is dependent on cathode to ground capacitance and the results are discussed in Sec. 4.

3. Overall R&D Effort to Define Experimental Parameters of the Detector

3.1 Computer Simulations Necessary for the Detector Design

We have developed a 2-D electrostatic program, which is able to simulate surfaces and wires.⁸ With this program we have simulated various aspects of the detector design.⁹ The program drifts electrons through the blind structure while including such effects as diffusion, correct drift velocity and the effect of the magnetic field. Figure 1 shows our nominal design. The design is surprisingly insensitive to misalignment; even if the individual blinds are randomly shifted up to 250 μm transversely relative to their axes, or randomly rotated by as much as 60° around the axis, one still obtains 100% transmission. With this program we have also studied gating effects, various edge effects, the time distribution of the photon feedback.⁹

Using an iterative technique,¹⁰ we have also calculated our sensitivity to the stringing tension and misalignment of the sense wires. We find that the anode wire is still stable in our structure even for tensions below 1 gram and that the gain changes by only 5% for a wire mispositioned by 250 μm .

3.2 Wire Aging and Its Solution for This Type of Detector

We have found that wire aging in gases doped with TMAE is more rapid than in usual drift chamber gases.¹¹ Our tests using a Fe-55 source, indicate that one would expect to lose a factor of two in gain after about 10^9 single photoelectrons have arrived on a 1 cm length of 7 μm diameter carbon wire operating with average total gain of about 2×10^5 in $\text{CH}_4 + \text{TMAE}$ (27°C) gas. Similar results have also recently been observed with UV sources by our group¹² and elsewhere.¹³ We have compared¹⁴ several different gases at 1 atm, and as is shown in Fig. 3, the aging rate in C_4H_{10} is about 12 times slower than that in CH_4 (taking a 50% gain drop as a measure). Going to lower pressures (10-40 Torr) the aging rate with C_4H_{10} gets even slower.¹³ It is useful to note that adding 1% and 3% of H_2 into $\text{CH}_4 + \text{TMAE}$ does not change the aging rate.¹⁴ Also we observe¹⁴ no sensitivity to gain on the wire (lowering it by factors 2 and 4), or the source intensity (changing it between 5-220 nA). We have also found that the wire aging rate in C_4H_{10} (no TMAE) was about as fast as in the $\text{C}_4\text{H}_{10} + \text{TMAE}$ gas.¹⁴

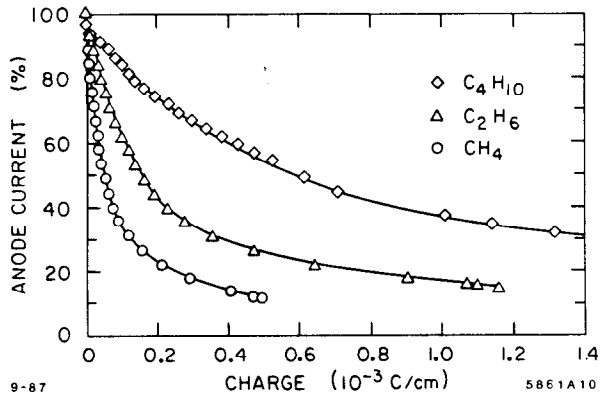


Fig. 3. Relative aging rate in CH_4 , C_2H_6 and C_4H_{10} with TMAE (26°C) at 1 atm and 7 μm diameter carbon wires.¹⁴

We have found two solutions to the wire aging problem.¹⁴ One method requires opening the detector to air (after purging), and washing the wires in an ultrasonic cleaner containing ethanol for a few minutes. In the second method, the detector is left in place and a small current is passed through each wire. The heating effect of the current, at an estimated temperature of $\sim 380^\circ \text{C}$ on the surface of the wire, evaporates the deposits and restores the gain.¹⁵ This evaporation has been directly observed in air under the microscope. Figure 4 shows repeated aging and heating treatment for one carbon wire. Figure 5 shows how the wire recovery depends on the value of the wire current. For example, a current of 11 mA (2 Watts) takes ~ 20 min. to clean the wires (wire breaks at 20 mA in the CH_4 gas). Although these measurements were performed in $\text{CH}_4 + \text{TMAE}$ gas, in the final detector we would prefer to heat the wire in CH_4 gas only, because TMAE might thermally decompose. We have, also successfully, treated wires previously aged in $\text{C}_4\text{H}_{10} + \text{TMAE}$ and C_4H_{10} (no TMAE). We are planning to incorporate the heating method in our final design, as frequent exposures of the detectors to air may cause problems (see Sec. 3.3). We also plan to incorporate the gating scheme to be insensitive to unwanted ionization.

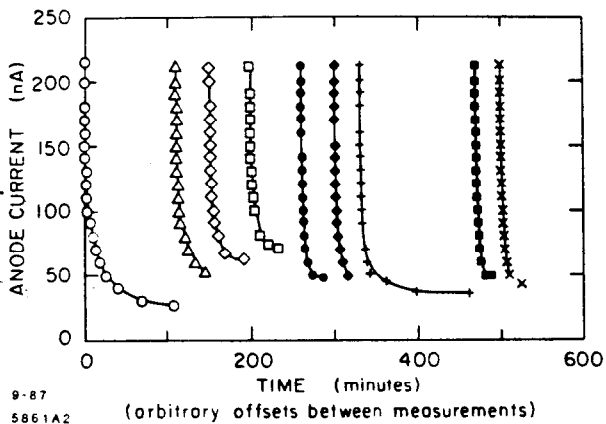


Fig. 4. Response to repeated aging (using an Fe-55 source) and curing of the same spot on 7 μm diameter carbon wire, $\text{CH}_4 + \text{TMAE}$ (27°C); the heat treatment used 11 mA (2 Watts) for 20 minute time interval (the first three aging cycles lasted only 3 minutes each, the rest took longer to cure). Each curve represents the cathode current during one aging cycle.¹⁴

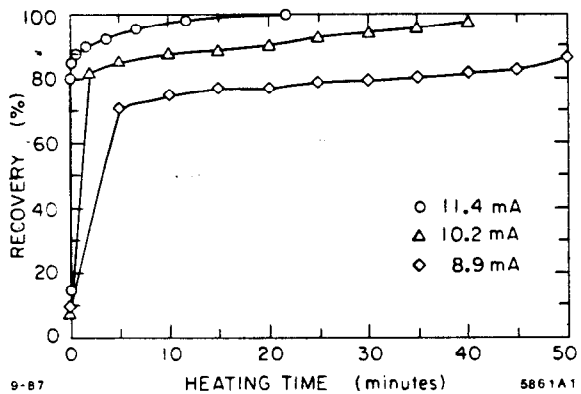


Fig. 5. Efficiency recovery as a function of curing current for 7 μm carbon wire, $\text{CH}_4 + \text{TMAE}$ (27°C).¹⁴

3.3 Surface Resistivity and Voltage Breakdown of G-10 in TMAE Environment

The present design of the detector uses G-10 as a material for spacers between blinds, for anode wire support, as well as for other parts of the detector. We have worried that the use of TMAE coupled with either some disaster with air, or frequent opening of detectors to air without sufficient waiting period to remove all traces of TMAE from the surfaces, would alter the surface resistivity sufficiently to cause a slow degradation of the electrical properties of the device. To address this question we have performed experiments to measure the surface resistivity and breakdown voltage of G-10¹⁶ (Figs. 6(a) and 6(b)). One can see that the surface resistivity of G-10 can decrease by four orders of magnitude if the TMAE is condensed on the surface and allowed to mix with air. During the same period the voltage breakdown limit drops by a factor of two to ≈ 900 V/mm. Of course, in a large system this value will have a certain distribution and one always suffers because of the tails of this distribution. Also, one can see that the detector recovers

very slowly from such a disaster, if at all. Therefore, we have been extremely conservative in designing the detector and have not allowed more than 200 V/mm across the G-10 surface within the detector. This has been accomplished by creating grooves in the G-10 spacers and anode wire PC-boards.

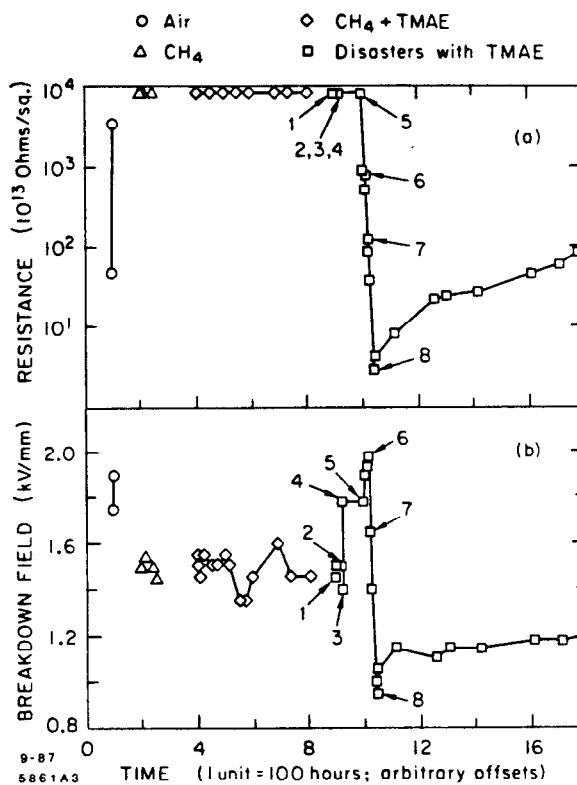


Fig. 6. (a) Surface resistivity, (b) Surface voltage breakdown as a function of various conditions: (1) vessel cold for two hours, $\text{CH}_4 + \text{TMAE}$ (26°C); (2) vessel warm again, flow CH_4 for 24 hours; (3) open vessel to air, start $\text{CH}_4 + \text{TMAE}$ immediately; (4) after 10 min., vessel warm; (5) switch temperature on vessel off, continue $\text{CH}_4 + \text{TMAE}$; (6) vessel cold for 18 hours, open it to air; (7) start heating the vessel, $\text{CH}_4 + \text{TMAE}$; (8) switch to CH_4 only gas, vessel warm, trying to recover.¹⁶

3.4 Corona Studies for Various Gases

We have performed extensive studies of corona problems in various gases¹⁷ for two reasons. The first was related to the high voltage field cage of the drift boxes, and the second was related to the detector. Because of the use of etched Cu-Be blinds the worry was that we would have a number of sharp points in the system which could trigger corona. The corona was studied in a controlled setup involving a needle with a 30 μm radius at the tip located 5 mm away from a flat electrode. Figure 7 shows the results of one such study in which the needle was connected to a negative voltage. One can see that the onset of corona is very fast and that the current step spans more than six orders of magnitude. The corona current step in methane is two orders of magnitude larger than, for instance, in C_5F_{12} . One can also see that the onset of corona in $\text{CH}_4 + \text{TMAE}$ gas occurs later than in CH_4 alone or even in air, which explains why these types of detectors are a bit more "nervous"

in CH_4 gas only, or in the initial air tests. Since CH_4 can support a very large corona current, this gas is rather prone to whisker growth, if the current lasts for any substantial length of time. Adding TMAE to CH_4 does not change the value of this current step. One should have a current trip level set below the corona current step value for the particular gas one is using. This can be difficult in large systems, where one usually must set the power supply current limit well above the corona step and one can end up with a number of "hot" spots. Reversing the polarity of the needle voltage produced similar curves to Fig. 7, although the thresholds for corona were observed at higher voltages.

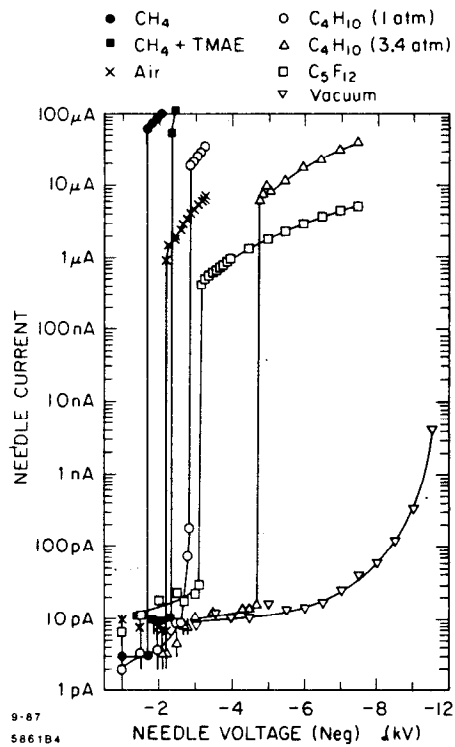


Fig. 7. Corona current for various gases; needle has about 30 μm radius at the tip, which is 5 mm away from a flat electrode; all gases are at 1 atm, and C_4H_{10} is also at 3.4 atm.¹⁷

Finally, we have found that such corona can act as a "polluter" of nearby surfaces. This can affect the work function of metals (making them photosensitive), or the transparency of quartz in the case of the drift box. For example, we have observed about a 25% U.V. transmission loss in a quartz sample placed a few centimeters away from the needle after about 10 Coulombs of total charge dose in the C_5F_{12} gas.

3.5 Wire Breaking in the Spark

We have found that 7 μm diameter carbon wires, tensioned at 6 grams, will break in a spark in air if the energy exceeds a value 0.8 ± 0.3 mJ (out of 25 wires, none broke below 0.5 mJ, and all broke above 1.4 mJ). It is interesting to note that this energy is lower than the value necessary to break 7.6 μm diameter tungsten wires strung at the same tension; in this case we measured 5.8 ± 2.5 mJ. The rather low value of the energy needed to break the carbon wire constrains the maximum value

of the cathode decoupling capacitor we can use to minimize crosstalk (see Section 4).

3.6 Measured Mechanical Characteristics of 7 μm Carbon Wires¹⁸

It is clear that the use of such thin wires in a large experiment is rather novel, and requires substantial R&D to answer a number of questions. We have measured the mean resistance of the 93 wires in the final detector to be $40.9 \pm 3.8 \text{ k}\Omega$ (about 10 cm wire length). Figure 8 shows that the wire diameter within each bundle varies causing a tail in the wire breaking and the resistance distributions. However, for each individual wire, the resistivity is uniform within 3% over a length of 25 cm. The fiber breaking tension has been measured to be 10.1 ± 2.1 grams, although the distribution has a nongaussian tail towards the lower values (see Sec. 3.7 on how to deal with this problem). The elongation of 10 cm long wires has been measured to be about 0.1 mm per gram. We have found the "elastic curve" to be linear for tensions up to 10 grams. Hence, stretching the wires at a tension of 5–6 grams seems safe, provided that we eliminate the weak wires (see Sec. 3.7).

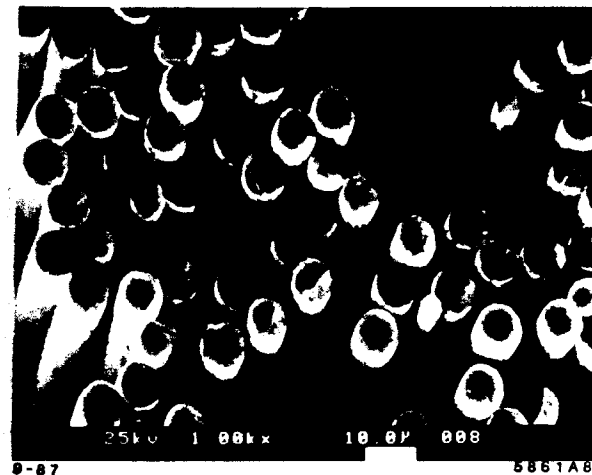


Fig. 8. Example of a bundle of 7 μm diameter carbon wires (notice that we have some weaker wires).

3.7 Wire Stretching Technique of 7 μm Carbon Wires

Stretching a large number of 7 μm carbon wires requires a careful procedure. We first pull the wire out if its bundle and glue a piece of hard paper to both ends. Figure 9 shows our stretching fixture. The prepared wire is laid down on two small tables, one of which is connected to a load cell¹⁹ which reads the tension. The wire is aligned by two bars with V-grooves, these are conducting and allow measurement of the wire resistance while being tensioned. We eliminate the weak wires by temporarily overtensioning each wire by 2 grams and also making a cut on the value of its resistance. After stretching to a tension of about 6 grams, we secure the wire with a tiny drop of fast-setting epoxy at four spots along the wire. We then use a conducting epoxy (H20-E made by Epotek, which was cured at 60°C for 12 hours) to make the electrical contact to the PC-board trace (a long term test to study the behavior of this epoxy is under way). We then cover the previous epoxies with a new coat of epoxy (Shell Epon 826 + Versamid 140,

cured at 50°C for 12 hours), which firmly secures the wire and is also TMAE resistant. At present we have stretched two full detectors using this procedure.

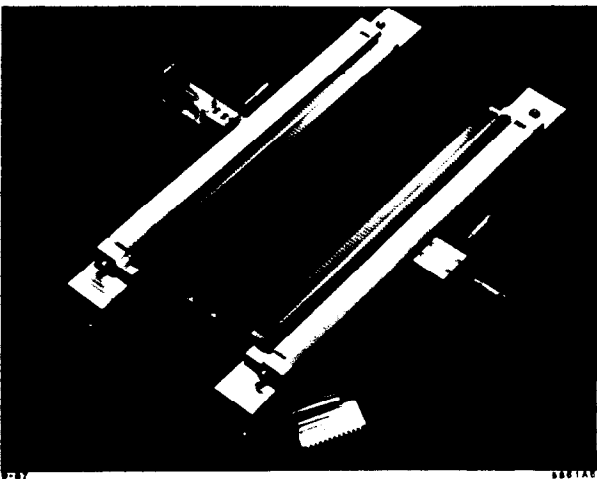


Fig. 9. Wire stretching fixture for the single electron CRID detector, together with the cathode. The tension is measured electrically by the load cell.¹⁹

3.8 Wire Tension Measuring Technique for the Final Detector

We have developed an elegant technique to measure the wire tensions in the detector.²⁰ We connect a sensitive amplifier²¹ across each wire and send the output to a frequency analyser. Using a gentle flow of N_2 gas we can induce mechanical vibration of the wire. A signal is obtained by placing a small magnet under the cathode. The typical range of resonating frequencies of the 10 cm long carbon wires in the final detector is about 4.5–5.5 kHz, i.e., far away from a typical low frequency noise spectrum. Figures 10(a) and 10(b) show the measured wire tensions for the wires in our first detector. One can see that by combining the tension measurement and the resistance measurement to correct the nominal value of wire diameter, the overall spread of the values is reduced. The measured tensions agree very well with the load cell measurements during the wire stretching. We plan to measure every cathode using this technique to check the performance of the load cell, as well as to study possible long term slippages of the wires (so far, after three months, we have observed no slippage).

4. The First Experimental Results With The Final Detector

We have operated the first detector at the nominal operating voltages (Fig. 1) for one month continuously in CH_4 gas. During this time, the monitored cathode current was consistent with zero at a 100 picoamperes sensitivity, indicating that the Cu-Be etched arrays do not have corona problems.

We have also measured the wire to wire crosstalk as a function of the cathode capacitance. This measurement is important because we want to minimize the crosstalk effects due to very large dE/dx signals caused by charged particles. We find that the crosstalk from one wire to a wire ten slots away (distant wire) is of opposite polarity, has the same time structure and is of magnitude 1.1% for 0.34 nF, and 0.5% for 4.5 nF compared to a primary signal. The measurement was done using a Fe-55 source which required a reduction in the operating voltages to prevent saturation. The primary signal had a pulse height of about 1200 mV, i.e., equivalent to about 10 photoelectrons at final operating voltages. Since a 4.5 nF capacitor

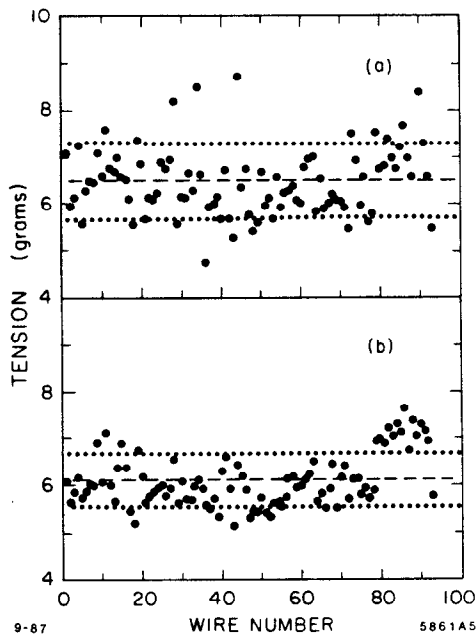


Fig. 10. Wire tension measured using the frequency analyzer, N_2 gas flow, amplifier and a magnet technique: (a) assume a fixed 7 μm wire diameter; (b) use a resistance measurement to correct for wire diameter variation (assume uniform density and resistivity).²⁰

value is rather dangerous from the wire breakage point of view, we presently plan to limit the value to 0.3 nF, and at the same time limit the cathode voltage to 1.7 kV (see Sec. 3.5).

Figure 11 shows the single electron pulse height spectrum in C_2H_6 gas for various cathode voltages as measured in the final detector. We used a tightly collimated continuous U.V. light source,²² attenuated to give only 50 Hz rate of single electrons on a 3–5 mm section of the wire. The spectrum was recorded using a LeCroy QVT pulse height spectrum analyzer operating in "Q-mode" with an internal gate 420 nsec long. The QVT threshold was set to its lowest setting of 1 mV, and the attenuation of the signal was carefully adjusted to be fully efficient for the lowest single electron pulse heights. The gain of our amplifier was measured to be 1.15 $\mu\text{V}/\text{electron}$ and the gain of a full signal chain was 2.2×10^{-3} QVT-channel/electron. We have corrected the visible gain for the full drift of positive ions in order to obtain the total gain on the wire. Figure 12 shows the results, where we plot the total gain corresponding to the peak value of each single electron pulse height spectrum. The noise in our system during this particular measurement was $\sigma_{\text{Noise}} \cong 2600$ electrons (the set-up was not yet final).

5. Conclusions

We have developed a workable technique to build the CRID single electron detectors using 7 μm carbon fibers. A number of problems, which looked initially insurmountable, were solved to our satisfaction. The operation of the detector was remarkably stable. We are, however, still concerned with the long term behavior of various critical parameters. We have the option of using thicker carbon wires (33 μm diameter) in case of difficulties with the thinner ones. This would cost us a factor of three in degradation of charge division resolution and require an additional R & D.

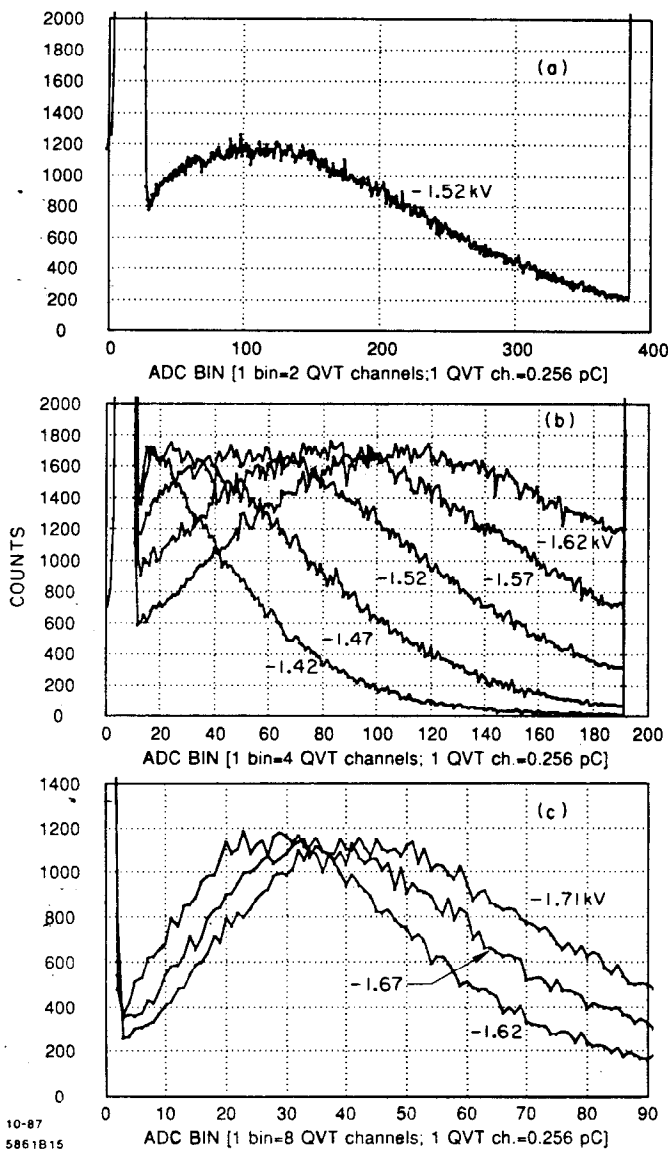


Fig. 11. Single electron pulse height spectrum in C_2H_6 gas (no TMAE) measured in the final CRID detector. Collimated U.V. source created 50 Hz rate of single electrons. Vary the cathode voltage, the rest of the detector voltages were as in Fig. 1. Use 16 dB attenuator in cases a, b, and 20 dB in case c.

Acknowledgements

We would like to extend thanks for engineering help to R. Shaw, A. Nuttall and G. Oxoby. For technical help, we would like to thank W. Chandler, D. Millican, R. Reif, H. Rogers and M. Pease.

References

1. F. Bird, S. Shapiro, V. Ashford, D. McShurley, R. Reif, D.W.G.S. Leith, S. Williams, IEEE Trans. Nucl. Sci. NS 33, 261, (1986) and SLAC-PUB 3790, 1985.
2. CRID-SLD Design Report #273, "Particle Identification (CRIDs)", June 16, 1987, RICH—Invited talk by J. Seguinot, Vienna Conf., 1986, and D. Bloch *et. al.*, London Conf., 1987.
3. G. Hallewell *et. al.*, submitted 1987 IEEE Symposium, SLAC-PUB-4405.
4. Blinds are made by PCM Products Inc., Titusville, FL 32780, USA.
5. N. Toge and M. Gaillard, "Space Charge Effect in the CRID Drift Box and a Gating Scheme", CRID Memo #16, 1986, unpublished.
6. E. Spencer *et. al.*, submitted IEEE Symposium, SLAC-PUB-4404.
7. V. Ashford *et. al.*, SLAC-PUB-4064, 1986.
8. S. Yellin, "Laplace and Electrostatics Program", CRID Memo #40, 1987, unpublished.
9. M. Gaillard, "Electrostatics Studies", CRID Memo #42, 1987, unpublished.
10. J. Va'vra, "Electrostatic Wire Stability in the CRID Electron Detector", CRID Memo #43, 1987, unpublished.
11. J. Va'vra, IEEE Trans. Nucl. Sci. NS 33 (1986) and SLAC-PUB 4116, 1986.
12. P. Coyle, "Drift Studies of the Physics Prototype", CRID Memo #41, 1987, unpublished.
13. C. Woody, 1987 IEEE Symposium and private communication.
14. J. Va'vra, "Summary on Wire Aging in TMAE Environment", CRID Memo #36, 1987, unpublished.
15. It was later pointed out to us by M. Atac that a similar technique was used 30 years ago to clean Geiger-Mueller counters, L. Shepard, Rev. Sci. Instr. 20, 217 (1949).
16. J. Va'vra, "Surface Resistivity and Voltage Breakdown of G-10 in TMAE Environment", CRID Memo #37, 1987, unpublished.
17. J. Va'vra, "Corona Studies for Various Gases", CRID Memo #38, 1987, unpublished.
18. TOHO RAYON CO., Tokyo, Japan; we use ST-3 6000 type of "sized" wire. Other manufacturers' quoted parameters worth mentioning are the wire density (1.77 g/cm^3) and a coefficient of thermal expansion ($-0.1 \times 10^{-6}/^\circ\text{C}$).
19. Load cell made by SENSO-TEC, Inc., 1200 Chesapeake Ave., Columbus, OH 43212.
20. R. Stephens, P. Rensing, J. Va'vra, "Wire Tension Measuring Technique for 7 μm Carbon Fibers to be Used in CRID Detector", CRID Memo #39, 1987, unpublished.
21. The amplifier circuit based on the OP-27 chip was suggested by G. Mundy, SLAC, 1987.
22. Hamamatsu deuterium lamp, model C1518.

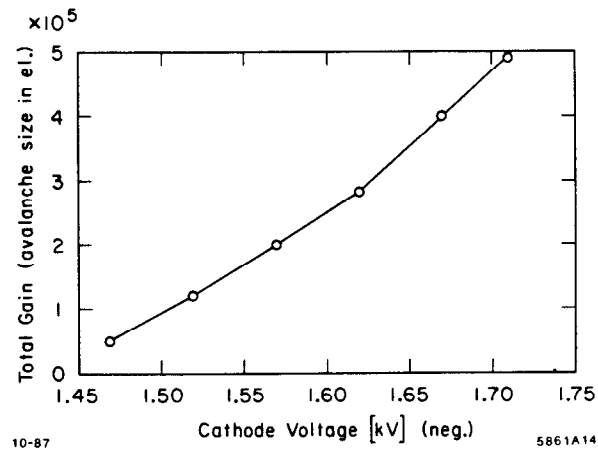


Fig. 12. Total gain corresponding to peak values of the single electron spectra as a function of the cathode voltage. The rest of detector voltages were as in Fig. 1.

6